

Search for excited spin-3/2 and spin-1/2 leptons at linear colliders

O. Cakir* and A. Ozansoy†

Ankara University, Faculty of Sciences,

Department of Physics, 06100, Tandogan, Ankara, Turkey

Abstract

We study the single production of excited spin-3/2 and spin-1/2 leptons in future high energy e^+e^- collisions. We calculate the production cross section and decay widths of excited spin-3/2 and spin-1/2 leptons according to their effective currents. We show that these possible new excited states can be probed up to the mass $m^* \sim \sqrt{s}$ depending on their couplings to leptons and gauge bosons. We present the angular distributions of final state particles as a measure to discriminate between an excited spin-3/2 and spin-1/2 lepton signal. The signals and the corresponding backgrounds are studied in detail to obtain attainable limits on masses and couplings of excited leptons at future linear colliders.

arXiv:0709.2134v1 [hep-ph] 13 Sep 2007

*Electronic address: ocakir@science.ankara.edu.tr

†Electronic address: aozansoy@science.ankara.edu.tr

I. INTRODUCTION

The replication of three fundamental fermion generations suggests the possibility that they are composite structures made up of more fundamental constituents. At a scale of constituent binding energies there should appear new interactions among quarks and leptons. Such interactions can appear by a constituent interchange or by exchange of a messenger particle. Excited leptons and quarks (l^*, q^*) appear as a consequence of the compositeness [1]. In the framework of composite models of quarks and leptons an excited spin-1/2 lepton is considered to be the lowest lying radial and orbital excitation, then excited spin-3/2 states are also expected to exist [2]. Composite quarks and leptons in the enlarged groups of the standard theory would also imply spin-3/2 quarks and leptons [3]. Further motivation for spin-3/2 particles comes from the supergravity (SUGRA) where spin-3/2 gravitino is as the superpartner of the graviton [4].

Phenomenologically an excited lepton can be considered to be a heavy lepton sharing leptonic quantum number with the corresponding ordinary lepton. Massive spin-3/2 excited states with the analogous heavy spin-1/2 excited one can be produced at future high energy colliders through their effective interactions with the ordinary leptons. Previous studies of production and decay properties of charged spin-3/2 leptons can be found in [2, 5, 6]. In electron-positron collisions excited spin-3/2 leptons can be produced in pairs, but it is limited kinematically by $m^* < \sqrt{s}/2$, while single production can reach masses as high as \sqrt{s} . An analysis of the production and decay processes of single heavy spin-3/2 leptons was performed in [6] in the frame of two phenomenological currents taking into account only the signal (without background consideration) coupled to Z -boson and W -boson.

Current direct limits on the masses of excited charged spin-1/2 leptons are: $m^* > 103.2$ GeV from pair production at LEP experiments [7] assuming non chiral transition couplings. $m^* > 255$ GeV from single production at HERA assuming chiral couplings for excited electron e^* [8]. Relatively small mass limits for single production of excited muon $m^* > 190$ GeV [7], and $m^* > 185$ GeV from single production of excited tau. The mass limits for excited neutrino from single production $m^* > 190$ GeV, and $m^* > 102.6$ GeV from pair production [9] assuming $f = -f'$. Relatively small mass limits are obtained for $f = f'$, where f and f' are the scaling factors for the gauge couplings of $SU(2)$ and $U(1)$. Indirect limits on the mass of excited spin-1/2 electron is $m^* > 310$ GeV from LEP experiment

assuming chiral couplings [10, 11].

In this study, we start with a transition magnetic type couplings between ordinary and excited spin-1/2 leptons, and three types of phenomenological currents of the spin-3/2 fields motivated by the new physics scale available at future high energy collisions. In the upcoming sections we present the branching rates of excited spin-3/2 and spin-1/2 electrons, the production cross sections depending on their masses at the available center of mass energies of future high energy e^+e^- colliders, namely International Linear Collider (ILC) [12] with $\sqrt{s} = 0.5$ TeV and Compact Linear Collider (CLIC) [13] with an optimal design energy of $\sqrt{s} = 3$ TeV. Finally, we compare the angular distributions of final state particles to discriminate between spin-3/2 and spin-1/2 excited electron signal from the corresponding background.

II. PHENOMENOLOGICAL CURRENTS

The interaction between a spin-1/2 excited electron, gauge boson ($V = \gamma, Z, W^\pm$) and the SM lepton is described by the effective current:

$$J_{1/2}^\mu = \frac{g_e}{2\Lambda} \bar{u}(k, 1/2) i\sigma^{\mu\nu} q_\nu (1 - \gamma_5) f_V u(p, 1/2) \quad (1)$$

where Λ is the scale of new physics responsible for the new interactions, k, p and q are the four-momentum of SM lepton, excited spin-1/2 electron and gauge boson, respectively. Electromagnetic coupling constant is given by $g_e = \sqrt{4\pi\alpha}$. f_V is the electroweak coupling parameter corresponding to a vector boson. In Eq. (1) $\sigma^{\mu\nu} = i(\gamma^\mu\gamma^\nu - \gamma^\nu\gamma^\mu)/2$ where γ^μ being the Dirac matrices. For an excited spin-1/2 electron, three decay channels are possible: radiative decay $e^* \rightarrow e\gamma$, neutral weak decay $e^* \rightarrow eZ$, charged weak decay $e^* \rightarrow \nu W$. If we neglect the SM lepton masses we find decay widths as

$$\Gamma(e^{*(1/2)} \rightarrow lV) = \frac{\alpha m^{*3}}{4\Lambda^2} f_V^2 (1 - \frac{m_V^2}{m^{*2}})^2 (1 + \frac{m_V^2}{2m^{*2}}) \quad (2)$$

where $f_\gamma = -(f + f')/2$, $f_Z = (-f \cot \theta_W + f' \tan \theta_W)/2$ and $f_W = f/\sqrt{2} \sin \theta_W$ for excited charged lepton. The parameters f and f' are determined by the composite dynamics, and they can be changed to q^2 -dependent form factors. In the literature, they are often taken as $f = f' = 1$ or $f = -f' = 1$ for $\Lambda = m^*$. The total decay width of the excited spin-1/2 electron is $\Gamma \simeq 1.9(6.9)$ GeV for $m^* = 0.3(1)$ TeV at $f = f' = 1$ and $\Lambda = m^*$. When we take

$f = -f' = 1$ the results for decay widths slightly change for smaller mass values, and we find the total decay width for e^* as $\Gamma \simeq 1.8(6.9)$ GeV at $\Lambda = m^* = 0.3(1)$ TeV. For these cases the total decay width of e^* depending on its mass can be found in Table I. The branching ratios of the excited spin-1/2 electrons into SM leptons and gauge bosons are given in Fig. 1. As seen from Fig. 1 charged current decays become dominant for higher mass values $m^* > 150$ GeV. Their relative importance depends on the gauge boson mass and couplings.

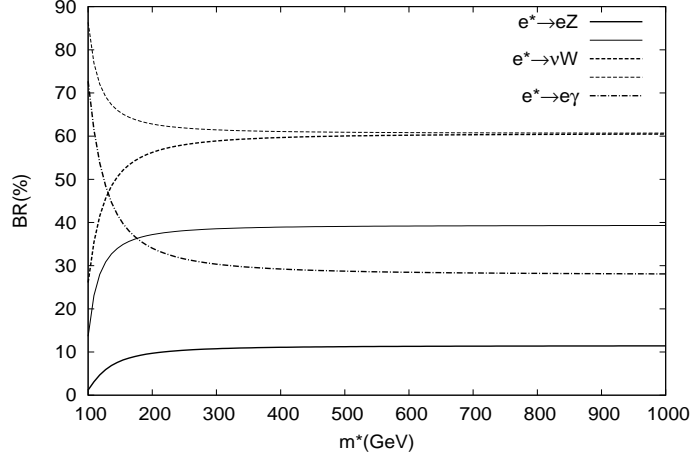


FIG. 1: The branching ratios (%) depending on the mass of excited spin-1/2 electron for $f = f' = 1$ (thick lines) for $f = -f' = 1$ (thin lines).

The phenomenological currents for the interactions among spin-3/2 excited electron, gauge boson and SM lepton are given by

$$J_1^\mu = g_e \bar{u}(k, 1/2)(c_{1V} - c_{1A}\gamma_5)u^\mu(p, 3/2) \quad (3)$$

$$J_2^\mu = \frac{g_e}{\Lambda} \bar{u}(k, 1/2)q_\lambda \gamma^\mu (c_{2V} - c_{2A}\gamma_5)u^\lambda(p, 3/2) \quad (4)$$

$$J_3^\mu = \frac{g_e}{\Lambda^2} \bar{u}(k, 1/2)q_\lambda i\sigma^{\mu\nu} q_\nu (c_{3V} - c_{3A}\gamma_5)u^\lambda(p, 3/2) \quad (5)$$

where $u^\mu(p, 3/2)$ represents the Rarita-Schwinger vector-spinor [14], c_{iV} and c_{iA} are the vector and axial vector couplings, the four momenta $q_\alpha = (p - k)_\alpha$. A spin-3/2 excited electron (e^*) decays via two-body process according to the phenomenological currents. The weak decay widths of excited spin-3/2 electrons for three different currents are given by

$$\Gamma_1(e^{*(3/2)} \longrightarrow lV) = \frac{\alpha}{48}(c_{1V}^2 + c_{1A}^2)m^* \frac{(1-\kappa)^2}{\kappa}(1+10\kappa+\kappa^2) \quad (6)$$

$$\Gamma_2(e^{*(3/2)} \longrightarrow lV) = \frac{\alpha}{48}(c_{2V}^2 + c_{2A}^2)m^* \left(\frac{m^*}{\Lambda}\right)^2 \frac{(1-\kappa)^4}{\kappa}(1+2\kappa) \quad (7)$$

$$\Gamma_3(e^{*(3/2)} \longrightarrow lV) = \frac{\alpha}{48}(c_{3V}^2 + c_{3A}^2)m^* \left(\frac{m^*}{\Lambda}\right)^4 (1-\kappa)^4(2+\kappa) \quad (8)$$

where $\kappa = (m_V/m^*)^2$ and m_V is the mass of the vector (W^\pm or Z) boson. The radiative decay widths of excited spin-3/2 electrons are given as

$$\Gamma_1(e^{*(3/2)} \longrightarrow e\gamma) = \frac{\alpha}{4}(c_{1V}^2 + c_{1A}^2)m^* \quad (9)$$

$$\Gamma_2(e^{*(3/2)} \longrightarrow e\gamma) = \frac{\alpha}{24}(c_{2V}^2 + c_{2A}^2)m^* \left(\frac{m^*}{\Lambda}\right)^2 \quad (10)$$

$$\Gamma_3(e^{*(3/2)} \longrightarrow e\gamma) = \frac{\alpha}{48}(c_{3V}^2 + c_{3A}^2)m^* \left(\frac{m^*}{\Lambda}\right)^4 \quad (11)$$

Here, one may note that the dimension five and six operators contributes as Λ^{-2} and Λ^{-4} to the decay widths, their relative importance is not essential when $\Lambda = m^*$. Taking $\Lambda = m^* = 0.5(1)$ TeV and $c_{iV} = c_{iA} = 0.5$ we find the total decay widths of the excited spin-3/2 electrons as $\Gamma_1 = 3.9(24.6)$ GeV, $\Gamma_2 = 2.7(22.2)$ GeV and $\Gamma_3 = 0.23(0.48)$ GeV for the currents J_1 , J_2 and J_3 , respectively. The decay widths of spin-3/2 e^* are shown in Table I. At equal couplings and $\Lambda = m^*$, the difference between the decay widths is due to the κ terms and different radiative contributions for each currents. The corresponding branching ratios are given in Fig. 2. For equal couplings and $\Lambda = m^*$ the branching ratios for the weak decays corresponding to the current J_1 and J_2 appear to be dominant for $m^* \gtrsim 200$ GeV. For the current J_3 radiative and weak decay channels with the same couplings have equal probability for large m^* .

III. CROSS SECTIONS

The high energy e^+e^- collisions provide an excellent environment to search for excited leptons. Spin-3/2 and spin-1/2 excited leptons can be produced at future e^+e^- colliders, namely ILC and CLIC. The Feynman diagrams for single production of excited positron (or electron) via the s -channel and t -channel γ, Z exchange are shown in Fig. 3. On the other

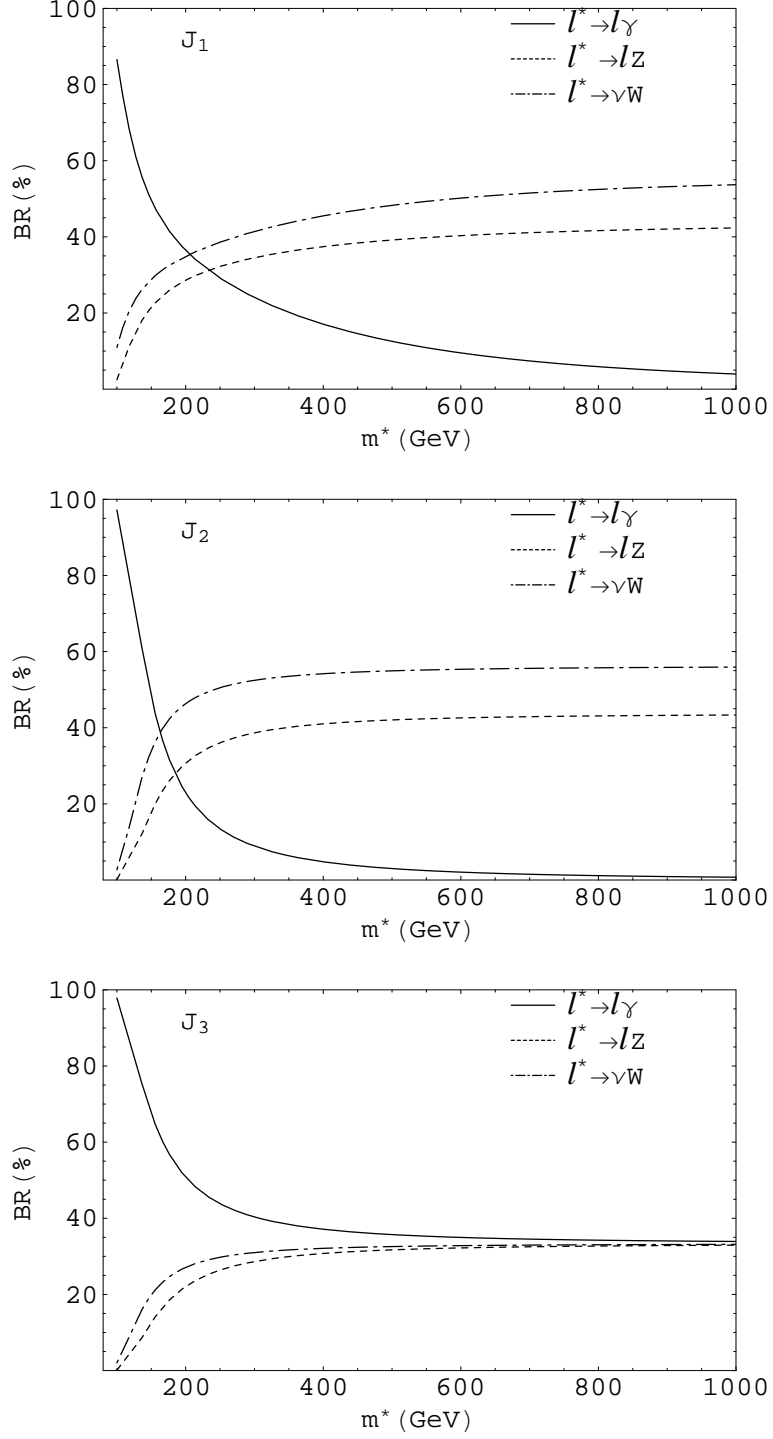


FIG. 2: The branching ratios as functions of excited spin-3/2 electron mass. The plots are given separately for J_1 , J_2 and J_3 currents.

TABLE I: Decay widths of excited spin-3/2 electrons with $c_V = c_A = 0.5$ depending on their mass values. Numbers in parenthesis show for the case $f = -f' = 1$ for spin-1/2 excited electron.

$m^*(\text{TeV})$	$\Gamma_{J(1/2)}$ (GeV)	$\Gamma_{J_1(3/2)}$ (GeV)	$\Gamma_{J_2(3/2)}$ (GeV)	$\Gamma_{J_3(3/2)}$ (GeV)
0.2	1.15 (1.03)	0.54	0.14	0.06
0.3	1.93 (1.85)	1.22	0.55	0.12
0.4	2.67 (2.61)	2.29	1.36	0.18
0.5	3.39 (3.35)	3.89	2.71	0.23
0.75	5.18 (5.15)	11.12	9.31	0.36
1.0	6.95 (6.93)	24.62	22.20	0.48
1.5	10.47(10.45)	78.89	75.24	0.73
2.0	13.98(13.97)	183.48	178.61	0.97
2.5	17.49(17.47)	355.16	349.07	1.22
3.0	20.99(20.98)	650.72	603.41	1.46

hand, single and pair production of excited muon or tau in the s -channel are also possible while their production in the t -channel leads to flavor changing neutral currents (FCNC).

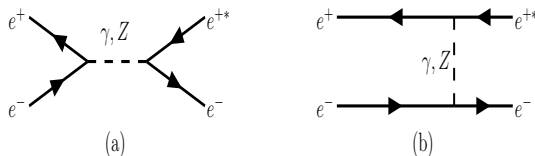


FIG. 3: Feynman diagrams for excited spin-3/2 or spin-1/2 positron production in e^+e^- collisions.

We calculate the cross sections for $e^+e^- \rightarrow e^{*+}e^-$ process for three currents J_1, J_2 and J_3 . Recently, spin-1/2 excited electron and neutrino have been studied at the ILC energy $\sqrt{s} = 0.5$ TeV in [15]. The $e^* \rightarrow e\gamma$ and $\nu^* \rightarrow eW$ signal have been searched for an easy identification and accurate measurements in a linear collider environment. The results show that spin-1/2 excited electron (neutrino) can be probed up to the mass $m^* = 350(450)$ GeV in the radiative (charged weak) decay channel when the coupling parameters are taken as $f = f' = 0.1$ for $\Lambda = m^*$.

The explicit calculations of the diagrams for excited spin-3/2 electrons lead to

$$\frac{d\sigma}{dt} = \frac{g_e^2}{24m^{*2} \pi s^2} \sum_{i,j=1,4} \frac{T_{ij}}{P_{ij}} \quad (12)$$

where we use the expressions T_{ij} and P_{ij} as given in the Appendix. Total cross sections as a function of excited electron mass are shown in Fig. 4 at $\sqrt{s} = 0.5$ and 3 TeV.

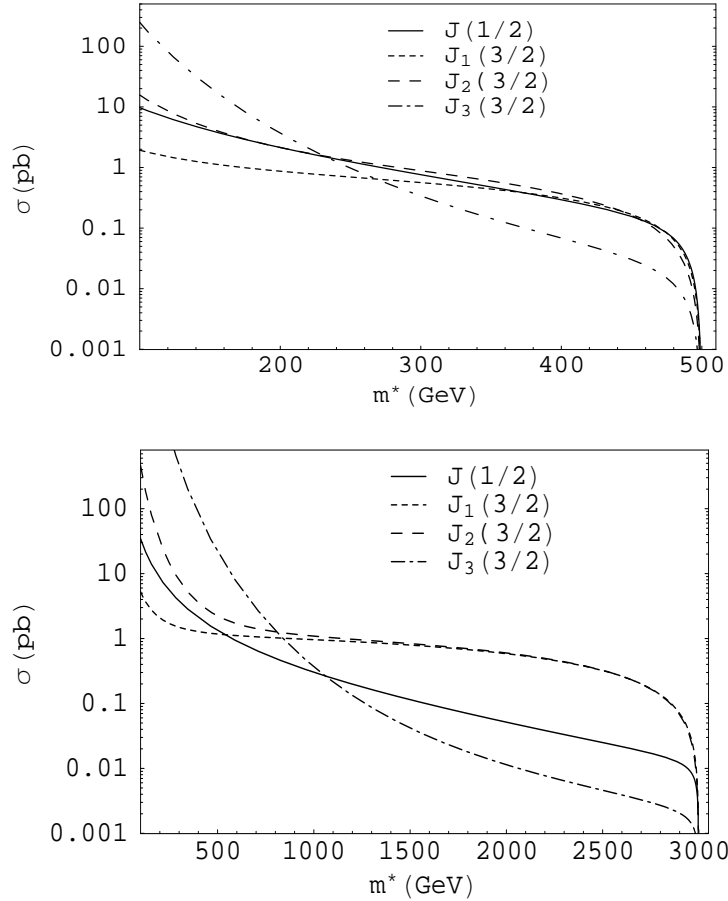


FIG. 4: Excited electron production cross section as a function of the mass at ILC energy $\sqrt{s} = 0.5$ TeV (upper) and CLIC energy $\sqrt{s} = 3$ TeV (lower). Solid, dotted, dashed and dot-dashed lines denote spin-1/2 and spin-3/2 with J_1 , J_2 , J_3 currents for $f = -f' = 1$ and $c_{iv}^Z = c_{iA}^Z = 0.5$, respectively.

One can see from Fig. 4 excited spin-3/2 electrons with current J_3 has a cross section larger than the other two currents when its mass below 1 TeV when produced at $\sqrt{s} = 3$ TeV. Depending on the couplings c_{iV}, c_{iA} the relative importance of three currents become more pronounced compared to the excited spin-1/2 electrons. In the analysis, we take into account only one coupling (i.e. coupling to one of the gauge bosons) that is kept free while

the others are assumed to vanish. In fact, there is no theoretical prediction on the total cross section for spin-3/2 single production. The Z -boson exchange in the s - and t -channel acts a heavy propagator as an effective form factor. On the other hand, if we choose $f = -f'$ photon decouples from the excited spin-1/2 electrons.

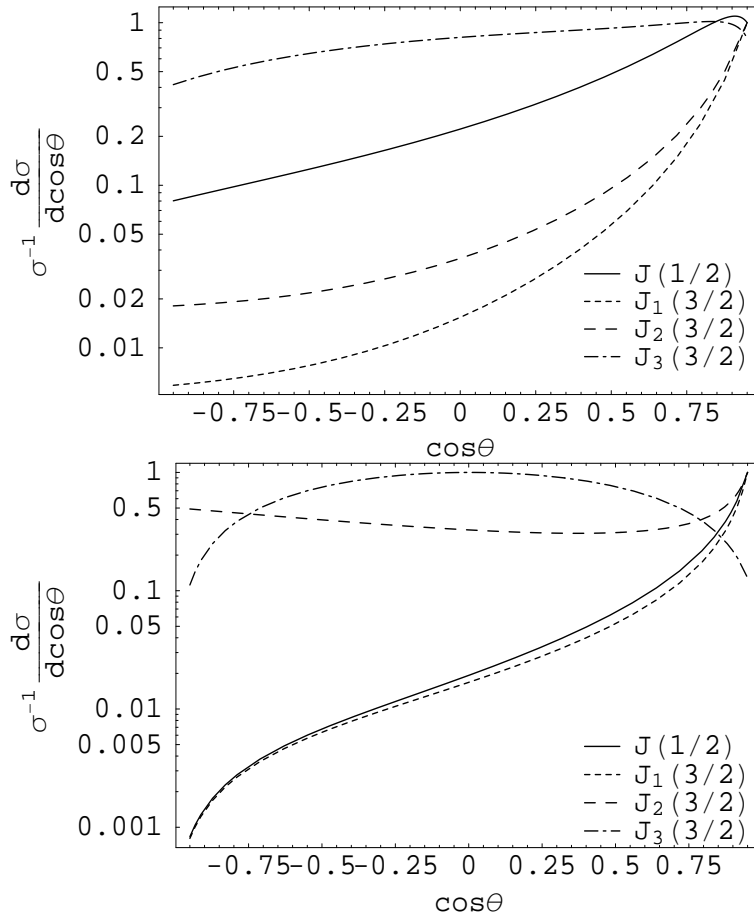


FIG. 5: The differential cross section as a function of the scattering angle for different spin-3/2 currents, and spin-1/2 excited electrons at (upper) $\sqrt{s} = 0.5$ TeV and (lower) $\sqrt{s} = 3$ TeV.

In order to differentiate the spin-3/2 and spin-1/2 excited electron signals we plot normalized differential cross sections as a function of $\cos\theta$ in Fig. 5. The excited spin-1/2 charged lepton is produced mostly in the forward direction, while excited spin-3/2 lepton shows different angular shape for the current J_3 than the others. For equal couplings, i.e. $c_{iV} = c_{iA}$, the normalized cross sections are not coupling dependent. For the final state we consider three decay channels of signal $e^* \rightarrow e\gamma$, $e^* \rightarrow eZ$ and $e^* \rightarrow \nu W$ for excited electron. In the first and second decay channels we obtain clear signal for a discovery, while the last decay channel for e^* has uncertainty due to the neutrino in the final state.

TABLE II: The cross sections for the signal and background after the cuts at e^+e^- colliders with 0.5 TeV. The signal cross section is given for $\Lambda = m^*$ and $c_{iV}^Z = c_{iA}^Z = 0.5$ for spin-3/2 and $f = -f' = 1$ for spin-1/2 excited electron.

$m^*(\text{GeV})$	$\sigma_S(\text{pb})$				$\sigma_B(\text{pb})$
	$J(1/2)$	$J_1(3/2)$	$J_2(3/2)$	$J_3(3/2)$	
200	2.14	0.87	2.13	3.68	1.47×10^{-2}
250	1.24	0.69	1.31	0.97	1.27×10^{-2}
300	0.76	0.56	0.88	0.34	1.26×10^{-2}
350	0.48	0.44	0.60	0.14	1.44×10^{-2}
400	0.29	0.31	0.37	0.07	1.73×10^{-2}
475	0.08	0.08	0.07	0.02	9.73×10^{-3}

In order to perceive the excited electron signals from the background we put kinematical cuts on the final state particles. The signal can be more pronounced over the background by applying suitable cuts. We consider the processes $e^+e^- \rightarrow e^-e^+\gamma$, $e^+e^- \rightarrow e^-e^+Z$ and $e^+e^- \rightarrow e^-\bar{\nu}W^+$ for the background. We calculate the background cross sections by using CalcHEP [16]. We apply the following acceptance cuts: $p_T^{e,\gamma} > 20$ GeV, $|\eta_{e,\gamma}| < 2.5$, $\Delta R_{(e^+e^-),(e^\pm\gamma)} > 0.4$, where p_T is the transverse momentum of final state detectable particle, η denotes pseudo rapidity and ΔR is the separation between two of them. The corresponding backgrounds are studied by applying the cuts on the transverse momentum and their pseudo rapidities of final state leptons and jets or missing transverse momentum when the SM neutrino is produced. After applying these cuts we find the cross section for the SM background as 1.93(0.16) pb, 0.11(0.03) pb and 0.92(0.46) pb at $\sqrt{s} = 0.5(3)\text{TeV}$ for $e^-e^+\gamma$, e^-e^+Z and $e^-\bar{\nu}W^+$, respectively. Furthermore, a way of extracting the excited electron signal from the background is to impose the cut $|m_{e\gamma} - m^*| < 25$ GeV on the invariant mass of the $e\gamma$ system and $|m_{eZ} - m^*| < 25$ GeV on the eZ invariant mass for the neutral weak decay channels of e^* . These cuts can be relaxed for higher values of the masses and couplings of e^* . For $m^* > 1.5$ TeV we apply a cut $m_{eV} > 1$ TeV for an easy detection of the signal. We present signal and background cross sections in Table II and III for different mass values taking equal couplings.

Fig. 6 shows the cross section for excited spin-3/2 and spin-1/2 electrons, when they

TABLE III: The cross sections for the signal and background after the cuts at e^+e^- colliders with 3 TeV. The signal cross section is given for $\Lambda = m^*$ and $c_{iV}^Z = c_{iA}^Z = 0.5$ for spin-3/2 and $f = -f' = 1$ for spin-1/2 excited electron.

$m^*(\text{GeV})$	$\sigma_S(\text{pb})$				$\sigma_B(\text{pb})$
	$J(1/2)$	$J_1(3/2)$	$J_2(3/2)$	$J_3(3/2)$	
250	5.45	1.69	14.4	1384.2	1.67×10^{-4}
500	1.33	1.17	2.22	21.71	8.26×10^{-4}
1000	0.30	0.96	1.08	0.37	3.24×10^{-4}
1500	0.11	0.79	0.84	0.04	3.67×10^{-4}
2000	0.05	0.06	0.06	0.01	1.66×10^{-2}
2500	0.025	0.032	0.032	0.004	1.66×10^{-2}
2750	0.017	0.17	0.17	0.003	1.66×10^{-2}

have electromagnetic couplings, depending on its mass for the ILC and CLIC energies. In order to determine the couplings $c_{iV}^\gamma, c_{iA}^\gamma$ we study the signal $e^* \rightarrow e\gamma$ and the corresponding background by applying the above mentioned cuts. In Table IV and V, we present the cross sections for signal and background for the chosen mass bin intervals at $\sqrt{s} = 0.5$ TeV and 3 TeV. Excited positrons (or electrons) with spin-3/2 can be distinguished from the spin-1/2 signal by searching for the angular distribution of associated electrons (or positrons) as shown in Fig. 7. Concerning the criteria $SS \geq 3$, and taking the couplings $c_V = c_A = 0.05$ the excited spin-3/2 electrons (having current J_3) can be observed up to 0.48 TeV and 2.0 TeV at ILC and CLIC energies as shown in Fig. 8. As can be seen from Fig. 8, for the other currents accessible range for the masses becomes enlarged.

For the analysis of the excited spin-3/2 and spin-1/2 electrons at linear colliders we define the statistical significance (SS) of the signal as

$$SS = \frac{\sigma_S}{\sqrt{\sigma_B}} \sqrt{\epsilon \cdot L}$$

where L_{int} is the integrated luminosity of the collider and ϵ is the efficiency to detect the signal in the chosen channel. In Fig. 6, discovery reach for spin-3/2 excited electrons are shown. With an integrated luminosity of $2 \times 10^5 \text{ pb}^{-1}$ the ILC can probe excited spin-3/2 electrons up to the mass 400 GeV if only the current J_3 is realized for $c_{3V}^Z = c_{3A}^Z = 0.05$. For

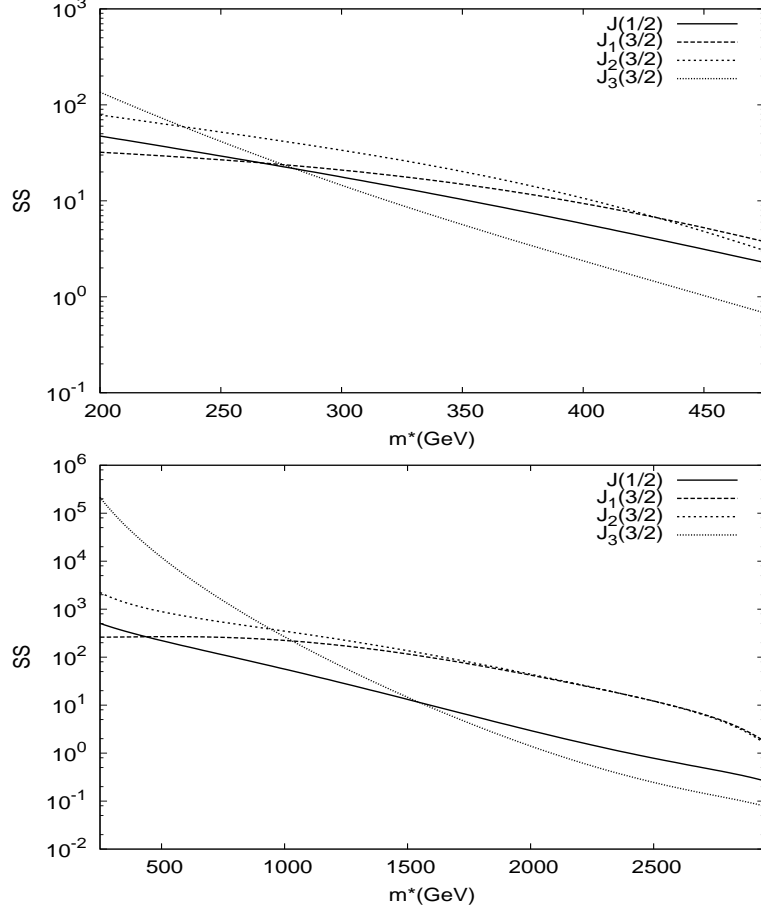


FIG. 6: Statistical significance for the excited electron signal (both for spin-1/2 and spin-3/2) at linear e^+e^- colliders with (upper) $\sqrt{s} = 0.5$ TeV and (lower) $\sqrt{s} = 3$ TeV.

TABLE IV: The cross sections for the signal and background after the cuts at e^+e^- colliders with 0.5 TeV. The signal cross section is given for $\Lambda = m^*$ and $c_{iV}^\gamma = c_{iA}^\gamma = 0.5$ for spin-3/2 and $f = f' = 1$ for spin-1/2 excited electron.

$m^*(\text{GeV})$	$\sigma_S(\text{pb})$				$\sigma_B(\text{pb})$
	$J(1/2)$	$J_1(3/2)$	$J_2(3/2)$	$J_3(3/2)$	
200	3.61	4.75	9.06	12.28	9.76×10^{-2}
250	2.22	4.27	6.28	3.46	1.17×10^{-1}
300	1.48	4.07	5.05	1.33	1.37×10^{-1}
350	1.03	4.00	4.41	0.65	1.52×10^{-1}
400	0.74	4.02	4.05	0.37	1.49×10^{-1}
475	0.45	4.16	3.75	0.21	5.05×10^{-2}

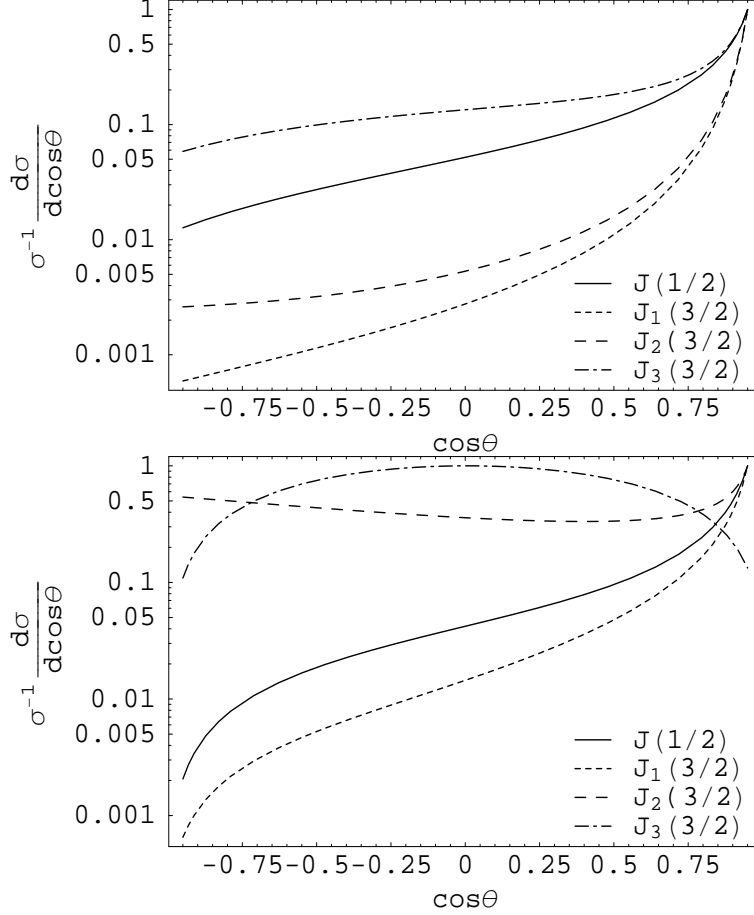


FIG. 7: The differential cross section as a function of the scattering angle for different spin-3/2 currents, and spin-1/2 excited electrons at (upper) $\sqrt{s} = 0.5$ TeV and (lower) $\sqrt{s} = 3$ TeV.

the same couplings other currents gives higher observability for the signal. At CLIC with $\sqrt{s} = 3$ TeV excited electrons can be probed up to the mass 2.0 TeV if their couplings are taken as $c_{3V}^Z = c_{3A}^Z = 0.05$.

IV. CONCLUSION

We consider only the gauge interactions of excited spin-3/2 and spin-1/2 electrons with the SM particles. In principle, excited leptons can also couples to SM leptons via contact interactions which may enlarge the discovery limits for the future colliders [17, 18]. If excited fermions having spin-1/2 or spin-3/2 are discovered singly or pairs at the forthcoming high energy colliders, there will be good reasons to separate them to understand the underlying dynamics which they obey. Our analysis show that spin-3/2 excited leptons can be easily

TABLE V: The cross sections for the signal and background after the cuts at e^+e^- colliders with 3 TeV. The signal cross section is given for $\Lambda = m^*$ and $c_{iV}^\gamma = c_{iA}^\gamma = 0.5$ for spin-3/2 and $f = -f' = 1$ for spin-1/2 excited electron.

$m^*(\text{GeV})$	$\sigma_S(\text{pb})$				$\sigma_B(\text{pb})$
	$J(1/2)$	$J_1(3/2)$	$J_2(3/2)$	$J_3(3/2)$	
250	2.52	1.04	38.54	4095.9	3.15×10^{-3}
500	0.63	0.33	2.93	63.5	1.75×10^{-3}
1000	0.15	0.15	0.37	0.99	1.37×10^{-3}
1500	0.07	0.12	0.17	0.10	9.19×10^{-4}
2000	0.04	0.11	0.13	0.02	3.31×10^{-2}
2500	0.03	0.11	0.11	0.009	3.31×10^{-2}
2750	0.02	0.11	0.11	0.007	3.31×10^{-2}

separated from the spin-1/2 ones by examining the normalized angular distributions in their single productions.

If polarized e^+ and e^- beams are used the chiral structure of the couplings can be identified and more precise measurements can be performed at the ILC and CLIC. Furthermore, if excited leptons are produced at resonance in $e\gamma$ collisions, which is an option for the linear colliders, the angular distribution of the decay products in a frame that they are at rest give valuable information about their spins. The prospects for the measurement of the spin of excited leptons will be shown elsewhere [19].

Excited leptons can come in three family, e^* , μ^* and τ^* , here we studied on the excited electron. The study for e^* can be enlarged by applying similar analysis to the excited muons and taus, and their neutrinos at the future high energy linear colliders.

V. APPENDIX

In equation (12) the T-terms T_{ij} and P-terms P_{ij} for the spin-3/2 excited electron interaction current J_1 are given as

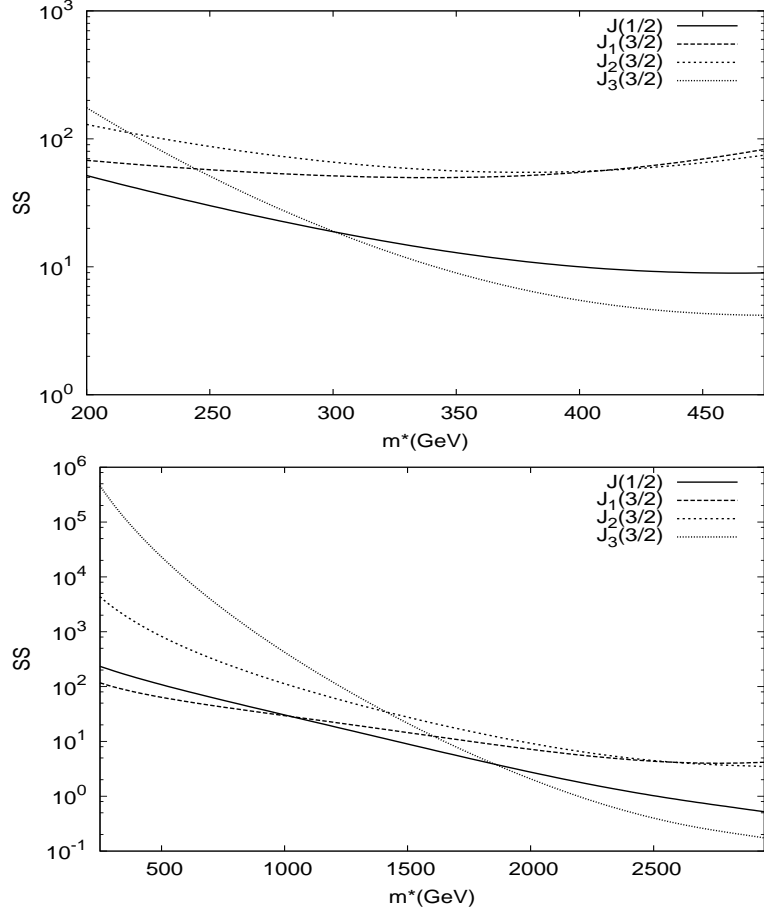


FIG. 8: The differential cross section as a function of the scattering angle for different spin-3/2 currents, and spin-1/2 excited electrons at (upper) $\sqrt{s} = 0.5$ TeV and (lower) $\sqrt{s} = 3$ TeV.

$$\begin{aligned}
T_{11}^{(1)} &= -g_e^2 (c_{1A}^\gamma{}^2 + c_{1V}^\gamma{}^2)(m^{*2} - s) (-t (s + t) + m^{*2} (2s + t)) \\
T_{12}^{(1)} &= [-g_e g_z (m_z^2 - s)(c_{1A}^\gamma (c_{1V}^Z c_A^f m^{*2} (m^{*2} - s - 2t) \\
&\quad + c_{1A}^Z c_V^f (st(s + t) + m^{*4}(2s + t) - m^{*2}(2s^2 + 2st + t^2)) + \\
&\quad c_{1V}^\gamma (c_{1A}^Z c_A^f (m^{*2} - s - 2t)s + c_{1V}^Z c_V^f (st(s + t) + m^{*4}(2s + t) \\
&\quad - m^{*2}(2s^2 + 2st + t^2)))]/2 \\
T_{13}^{(1)} &= [-g_e^2 (c_{1A}^\gamma{}^2 + c_{1V}^\gamma{}^2)(m^{*4} + st)(s + t) - m^{*2}(s^2 + t^2)]/2 \\
T_{14}^{(1)} &= [g_e g_z (c_A^f (c_{1V}^\gamma c_{1A}^Z + c_{1A}^\gamma c_{1V}^Z) \\
&\quad - c_V^f (c_{1A}^\gamma c_{1A}^Z + c_{1V}^\gamma c_{1V}^Z))((m^{*4} + st)(s + t) - m^{*2}(s^2 + t^2)]/4 \\
T_{22}^{(1)} &= [-g_z^2 (4c_{1A}^Z c_{1V}^Z c_A^f c_V^f m^{*2} s (m^{*2} - s - 2t) + \\
&\quad (c_{1A}^Z{}^2 + c_{1V}^Z{}^2)(c_A^{f2} + c_V^{f2}) (m^{*2} - s) (-t(s + t) + m^{*2}(2s + t)))]/4 \\
T_{23}^{(1)} &= [g_e g_z (c_A^f (c_{1V}^\gamma c_{1A}^Z + c_{1A}^\gamma c_{1V}^Z) - \\
&\quad c_V^f (c_{1A}^\gamma c_{1A}^Z + c_{1V}^\gamma c_{1V}^Z)) (m_z^2 - s) ((m^{*4} + st)(s + t) - m^{*2}(s^2 + t^2)]/4 \\
T_{24}^{(1)} &= [-g_z^2 (-4c_{1A}^Z c_{1V}^Z c_A^f c_V^f + \\
&\quad (c_{1A}^Z{}^2 + c_{1V}^Z{}^2)(c_A^{f2} + c_V^{f2})(m^{*4}(3s - t) + st(s + t) + m^{*2}(-3s^2 + t^2)))]/8 \\
T_{34}^{(1)} &= [-g_e g_z ((c_{1A}^\gamma (c_{1V}^Z c_A^f m^{*2} (m^{*2} - 2s - t)t \\
&\quad + c_{1A}^Z c_V^f (-m^{*2} + t)(s(s + t) - m^{*2}(s + 2t))) \\
&\quad + (c_{1V}^\gamma (c_{1A}^Z c_A^f m^{*2} (m^{*2} - 2s - t)t \\
&\quad + c_{1V}^Z c_V^f (-m^{*2} + t)(s(s + t) - m^{*2}(s + 2t)))))]/2 \\
T_{33}^{(1)} &= -g_e^2 (c_{1A}^\gamma{}^2 + c_{1V}^\gamma{}^2)(m^{*2} - t) (-s (s + t) + m^{*2} (s + 2t)) \\
T_{44}^{(1)} &= [g_z^2 (4c_{1A}^Z c_{1V}^Z c_A^f c_V^f m^{*2} t (-m^{*2} + 2s + t) - \\
&\quad (c_{1A}^Z{}^2 + c_{1V}^Z{}^2)(c_A^{f2} + c_V^{f2})(m^{*2} - t)(-s(s + t) + m^{*2}(s + 2t)))]/4
\end{aligned}$$

and

$$\begin{aligned}
P_{11}^{(1)} &= s^2, \quad P_{12}^{(1)} = s((m_z^2 - s)^2 + m_z^2 \Gamma_z^2), \quad P_{13}^{(1)} = st, \quad P_{14}^{(1)} = s(m_z^2 - t), \\
P_{22}^{(1)} &= (m_z^4 + s^2 + m_z^2(-2s + \Gamma_z^2)), \\
P_{23}^{(1)} &= t(m_z^4 + s^2 + m_z^2(-2s + \Gamma_z^2)), \quad P_{24}^{(1)} = (m_z^2 - t)(m_z^4 + s^2 + m_z^2(-2s + \Gamma_z^2)), \\
P_{34}^{(1)} &= (m_z^2 - t)t, \\
P_{33}^{(1)} &= t^2, \quad P_{44}^{(1)} = (m_z^2 - t)^2
\end{aligned}$$

The T_{ij} and P_{ij} terms for the current J_2 are given by

$$\begin{aligned}
T_{11}^{(2)} &= [-g_e^2 (c_{2A}^{\gamma^2} + c_{2V}^{\gamma^2})(m^{*2} - s)^2 (-s^2 - 2st - 2t^2 + m^{*2}(s + 2t))]/2\Lambda^2 \\
T_{12}^{(2)} &= [g_e g_z (m^{*2} - s)^2 (s - m_z^2) ((c_{2A}^{\gamma} (c_{2V}^Z c_A^f s(m^{*2} - s - 2t) \\
&\quad + c_{2A}^Z c_V^f (-s^2 - 2st - 2t^2 + m^{*2}(s + 2t))) \\
&\quad + c_{2V}^{\gamma} (c_{2A}^Z c_A^f s(m^{*2} - s - 2t) + c_{2V}^Z c_V^f (-s^2 - 2st - 2t^2 + m^{*2}(s + 2t)))]/4\Lambda^2 \\
T_{13}^{(2)} &= [-g_e^2 (c_{2A}^{\gamma^2} + c_{2V}^{\gamma^2})(m^{*2} - s - t)(s + t)(m^{*4} - st - m^{*2}(s + t))]/2\Lambda^2 \\
T_{14}^{(2)} &= [-g_e g_z (c_A^f (c_{2V}^{\gamma} c_{2A}^Z + c_{2A}^{\gamma} c_{2V}^Z) \\
&\quad + c_V^f (c_{2A}^{\gamma} c_{2A}^Z + c_{2V}^{\gamma} c_{2V}^Z))(m^{*2} - s - t)(s + t)(m^{*4} - st - m^{*2}(s + t))]/4\Lambda^2 \\
T_{22}^{(2)} &= [-g_z^2 (m^{*2} - s)^2 (-4c_{2A}^Z c_{2V}^Z c_A^f c_V^f s(-m^{*2} + s + 2t) + \\
&\quad (c_{2A}^{Z^2} + c_{2V}^{Z^2})(c_A^{f2} + c_V^{f2}) (-s^2 - 2st - 2t^2 + m^{*2}(s + 2t))]/8\Lambda^2 \\
T_{23}^{(2)} &= [-g_e g_z (c_A^f (c_{2V}^{\gamma} c_{2A}^Z + c_{2A}^{\gamma} c_{2V}^Z) + c_V^f (c_{2A}^{\gamma} c_{2A}^Z + c_{2V}^{\gamma} c_{2V}^Z) (m_z^2 - s) \\
&\quad (s + t)(-m^{*2} + s + t)(-m^{*4} + st + m^{*2}(s + t)))]/4\Lambda^2 \\
T_{24}^{(2)} &= [-g_z^2 (4c_{2A}^Z c_{2V}^Z c_A^f c_V^f + (c_{2A}^{Z^2} + c_{2V}^{Z^2})(c_A^{f2} + c_V^{f2}) (m_z^2 - s) \\
&\quad (-m^{*2} + s)(-2m^{*4} s + m^{*4}(s - t) + st(s + t) + m^{*2}(s + t)^2)]/8\Lambda^2 \\
T_{34}^{(2)} &= [g_e g_z (c_{2A}^{\gamma} (c_{2V}^Z c_A^f (m^{*2} - 2s - t)t + c_{2A}^Z c_V^f (-2s^2 - 2st - t^2 + m^{*2}(2s + t))) \\
&\quad + (c_{2V}^{\gamma} (c_{2A}^Z c_A^f (m^{*2} - 2s - t)t + c_{2V}^Z c_V^f (-2s^2 - 2st - t^2 + m^{*2}(2s + t))))]/4\Lambda^2 \\
T_{33}^{(2)} &= [-g_e^2 (c_{2A}^{\gamma^2} + c_{2V}^{\gamma^2})(m^{*2} - t)^2 (-2s^2 - 2st - t^2 + m^{*2}(2s + t))]/2\Lambda^2 \\
T_{44}^{(2)} &= [-g_z^2 (m^{*2} - t)^2 (4c_{2A}^Z c_{2V}^Z c_A^f c_V^f (m^{*2} - 2s - t) t \\
&\quad + (c_{2A}^{Z^2} + c_{2V}^{Z^2})(c_A^{f2} + c_V^{f2})(-2s^2 - 2st - t^2 + m^{*2}(2s + t))]/8\Lambda^2
\end{aligned}$$

and

$$\begin{aligned}
P_{11}^{(2)} &= s^2, \quad P_{12}^{(2)} = (m_z^4 s + s^3 + m_z^2(-2s^2 + \Gamma_z^2)), \quad P_{13}^{(2)} = st, \\
P_{14}^{(2)} &= s(m_z^2 - t), \quad P_{22}^{(2)} = 4(m_z^4 + s^2 + m_z^2 s(-2s + \Gamma_z^2)), \\
P_{23}^{(2)} &= t(m_z^4 + s^2 + m_z^2(-2s + \Gamma_z^2)), \quad P_{24}^{(2)} = (m_z^2 - t)(m_z^4 + s^2 + m_z^2(-2s + \Gamma_z^2)), \\
P_{34}^{(2)} &= (-m_z^2 + t)t, \\
P_{33}^{(2)} &= t^2, \quad P_{44}^{(2)} = (m_z^2 - t)^2
\end{aligned}$$

The T_{ij} and P_{ij} terms for the current J_3 are given by

$$\begin{aligned}
T_{11}^{(3)} &= [-g_e^2 (c_{3A}^\gamma)^2 + c_{3V}^{\gamma 2}) (m^{*2} - s)^2 (m^{*4} + 2t(s+t) - m^{*2}(s+2t))] / 2\Lambda^4 \\
T_{12}^{(3)} &= [-g_e g_z (m^{*2} - s)^2 (s - m_z^2) ((c_{3A}^\gamma (c_{3V}^Z c_A^f m^{*2} (m^{*2} - s - 2t) \\
&\quad - c_{3A}^Z c_V^f (m^{*4} + 2t(s+t) - m^{*2}(s+2t))) \\
&\quad + c_{3V}^\gamma (c_{3A}^Z c_A^f m^{*2} s (m^{*2} - s - 2t) - c_{3V}^Z c_V^f (m^{*4} + 2t(s+t) - m^{*2}(s+2t)))] / 4\Lambda^2 \\
T_{13}^{(3)} &= [g_e^2 (c_{3A}^\gamma)^2 + c_{3V}^{\gamma 2}) (m^{*2} - s - t) t s] / 2\Lambda^4 \\
T_{14}^{(3)} &= [g_e g_z (c_A^f (c_{3V}^\gamma c_{3A}^Z + c_{3A}^\gamma c_{3V}^Z) - c_V^f (c_{3A}^\gamma c_{3A}^Z + c_{3V}^\gamma c_{3V}^Z)) (m^{*2} - s - t) t (st)] / 4\Lambda^4 \\
T_{22}^{(3)} &= [-g_z^2 (m^{*2} - s)^2 (4c_{3A}^Z c_{3V}^Z c_A^f c_V^f m^{*2} s (-m^{*2} + s + 2t) + \\
&\quad (c_{3A}^Z)^2 + c_{3V}^Z)^2) (c_A^{f2} + c_V^{f2}) (m^{*4} + 2s(s+t) - m^{*2}(2s+t))] / 8\Lambda^4 \\
T_{23}^{(3)} &= [g_e g_z s^2 (c_A^f (c_{3V}^\gamma c_{3A}^Z + c_{3A}^\gamma c_{3V}^Z) - c_V^f (c_{3A}^\gamma c_{3A}^Z + c_{3V}^\gamma c_{3V}^Z) \\
&\quad (m_z^2 - s) t (-m^{*2} + s + t)] / 4\Lambda^4 \\
T_{24}^{(3)} &= [-g_z^2 (-4c_{3A}^Z c_{3V}^Z c_A^f c_V^f + (c_{3A}^Z)^2 + c_{3V}^Z)^2) (c_A^{f2} + c_V^{f2}) \\
&\quad (m_z^2 - s) s^2 t^2 (-m^{*2} + s + t)] / 8\Lambda^4 \\
T_{34}^{(3)} &= [-g_e g_z (m^{*4} - 6m^{*2}t + t^2) (c_{3A}^\gamma (c_{3V}^Z c_A^f m^{*2} (-m^{*2} + 2s + t) \\
&\quad + c_{3A}^Z c_V^f (m^{*4} + 2s(s+t) - m^{*2}(2s+t))) \\
&\quad + (c_{3V}^\gamma (c_{3A}^Z c_A^f m^{*2} (-m^{*2} + 2s + t) + c_{3V}^Z c_V^f (m^{*4} + 2s(s+t) - m^{*2}(2s+t)))] / 4\Lambda^4 \\
T_{33}^{(3)} &= [-g_e^2 (c_{3A}^\gamma)^2 + c_{3V}^{\gamma 2}) (m^{*2} - t)^2 (m^{*4} + 2s(s+t) - m^{*2}(2s+t))] / 2\Lambda^4 \\
T_{44}^{(3)} &= [-g_z^2 (4c_{3A}^Z c_{3V}^Z c_A^f c_V^f m^{*2} (m^{*2} - t)^2 (-m^{*2} + 2s + t) t \\
&\quad + (c_{3A}^Z)^2 + c_{3V}^Z)^2) (c_A^{f2} + c_V^{f2}) (m^{*4} + 2s(s+t) - m^{*2}(2s+t))] / 8\Lambda^4
\end{aligned}$$

and

$$\begin{aligned}
P_{11}^{(3)} &= s, \quad P_{12}^{(3)} = (m_z^4 s + s^3 + m_z^2 (-2s^2 + \Gamma_z^2)), \quad P_{13}^{(3)} = 1, \\
P_{14}^{(3)} &= (t - m_z^2), \quad P_{22}^{(3)} = ((m_z^2 - s)^2 + m_z^2 \Gamma_z^2), \\
P_{23}^{(3)} &= ((m_z^2 - s)^2 + m_z^2 \Gamma_z^2), \quad P_{24}^{(3)} = (m_z^2 - t) (m_z^4 + s^2 + m_z^2 (-2s + \Gamma_z^2)), \\
P_{34}^{(3)} &= (m_z^2 - t), \\
P_{33}^{(3)} &= t, \quad P_{44}^{(3)} = (m_z^2 - t)^2
\end{aligned}$$

Acknowledgments

This work was partially supported by the Turkish State Planning Organization (DPT) under grant No DPT-2006K-120470 and the Turkish Atomic Energy Authority (TAEK) under grant No VII-B.04.DPT.1.05.

-
- [1] H. Terazawa, Y. Chikashige, and K. Akama, Phys. Rev. D **15**, 480 (1977); Y. Ne'eman, Phys. Lett. **82B** 69 (1969); H. Terazawa, M. Yasue, K. Akama, and M. Hayashi, Phys. Lett. **112B**, 387 (1982)
 - [2] J. Leite Lopes, J. A. Martins Simoes, and D. Spehler, Phys. Lett. **94B**, 367 (1980); Phys. Rev. D **23**, 797 (1981); **25**, 1854 (1982)
 - [3] Y. Tosa and R. E. Marshak, Phys. Rev. D **32** 774 (1985)
 - [4] D. Z. Freedman, P. van Nieuwenhuizen and S. Ferrara, Phys. Rev. D **13** (1976) 3214
 - [5] S. R. Choudhury, R. G. Ellis, G. C. Joshi, Phys. Rev. D **31**, 2390 (1985).
 - [6] F. M. L. Almeida et al., Phys. Rev. D **53**, 7 (1996).
 - [7] G. Abbiendi et al., Phys. Lett. B **544** 57-72 (2002).
 - [8] C. Adloff et al., Phys. Lett. B **548** 35-44 (2002).
 - [9] P. Achard et. al., Phys. Lett. B **568** 23-24 (2003).
 - [10] P. Achard et. al., Phys. Lett. B **531** 39-51 (2003).
 - [11] W. -M. Yao et. al., J. Phys. G **33**, 1 (2006).
 - [12] G. A. Loew, Report from the ILC technical review committee, Slac-pub-10024 (2003); A comprehensive information about the future linear colliders can be found at the URL: <http://www.linearcollider.org>
 - [13] R. W. Assmann et al.; The CLIC Study Team, a 3 TeV e^+e^- linear collider based on CLIC Technology CERN-2000-008, Geneva 2000; E. Accomondo et al.; Report of the CLIC Physics Working Group, CERN-2004-005, Geneva 2004; hep-ph/0412251
 - [14] W. Rarita, J. Schwinger, Phys. Rev. **60**, 61 (1941).
 - [15] O.Cakir, A.Yilmaz and S. Sultansoy, Phys. Rev. D **70**, 075011 (2004); O.Cakir, I. Turk Cakir and Z. Kirca, Phys. Rev. D **70**, 075017 (2004).
 - [16] A.Pukhov et al, Preprint INP MSU 98-41/542; arXiv: hep-ph/9908288; A.Pukhov arXiv:

hep-ph/0412191.

- [17] U. Baur, M. Spira and P. M. Zerwas, *Phys. Rev. D* **42**, 815 (1990).
- [18] O. Cakir et al., *Eur. Phys. J. C* **32**, s02, 1 (2003).
- [19] O. Cakir, A. Ozansoy, Prospects for the measurements of the spin of excited leptons at linear colliders, in preperation (2007).